Therapeutics, Targets, and Chemical Biology

Cancer Research

Circadian Regulation of mTOR by the Ubiquitin Pathway in Renal Cell Carcinoma

Hiroyuki Okazaki[1], Naoya Matsunaga[1], Takashi Fujioka[1], Fumiyasu Okazaki[1], Yui Akagawa[1], Yuuya Tsurudome[1], Mayumi Ono[2], Michihiko Kuwano[2], Satoru Koyanagi[1], and Shigehiro Ohdo[1]

Abstract

Circadian clock systems regulate many biologic functions, including cell division and hormone secretion in mammals. In this study, we explored the effects of circadian control on the pivot cell growth regulatory mTOR, the activity of which is deregulated in tumor cells compared with normal cells. Specifically, we investigated whether the antitumor effect of an mTOR inhibitor could be improved by changing its dosing schedule in RenCa tumor-bearing mice. Active, phosphorylated mTOR displayed a 24-hour rhythm, and levels of total mTOR protein (but not mRNA) also showed a circadian rhythm in RenCa tumor masses. Through investigations of the oscillation mechanism for mTOR expression, we identified the ubiquitination factor Fbxw7 as an mTOR regulator that oscillated in its expression in a manner opposite from mTOR. Fbxw7 transcription was regulated by the circadian regulator D-site–binding protein. Notably, administration of the mTOR inhibitor everolimus during periods of elevated mTOR improved survival in tumor-bearing mice. Our findings demonstrate that the circadian oscillation of mTOR activity is regulated by circadian clock systems, which influence the antitumor effect of mTOR inhibitors. *Cancer Res; 74(2); 543–51. ©2013 AACR.*

Introduction

The circadian clock system controls various biologic functions in mammals. The master pacemaker of the mammalian clock is situated in the suprachiasmatic nuclei of the hypothalamus (1). Circadian clocks consist of interconnected transcription–translation feedback loops. The CLOCK–BMAL1 protein complex drives the transcription of *Per*, *Cry*, and *Dec*, which act as repressors by interacting with CLOCK/BMAL1 (2–4). This complex also activates the transcription of *Dbp* and *Rorα*, which act as transcriptional activators by binding to D sites and ROR-specific response elements, respectively (5, 6). These mechanisms create a periodically repeated activation/repression cycle of clock-controlled genes in peripheral tissues, including tumor tissues (7, 8).

The circadian rhythms of biologic functions are thought to affect the efficacy and/or toxicity of drugs. For example, in cancer therapy, the circadian rhythms of metabolic enzymes and signal transduction proteins targeted by antitumor drugs influence the effect of these drugs (9–11). It has been suggested that administration of drugs at an appropriate time of the day could improve the outcome of pharmacotherapy. However, many antitumor drugs are still administered without regard to the time of the day. Elucidating the chronotherapeutic mechanism underlying the dosing time dependency of the antitumor effects of these agents could improve the chronopharmacotherapy for cancer treatments.

mTOR is a member of the phosphoinositide 3-kinase–related kinase (PIKK) family and is a critical regulator of proliferation (12, 13). mTOR plays a key role in cell-cycle progression and proliferation; therefore, inhibition of mTOR induces cell-cycle arrest and apoptosis. mTOR also regulates cell metabolism. mTOR-signaling activity is higher in tumor cells than in normal cells; thus, mTOR inhibitors such as everolimus have attracted attention as new antitumor drugs (14–16). mTOR is activated by various growth factors, and it promotes cell growth through phosphorylation of ribosomal protein S6K (P70S6K) and eukaryotic initiation factor 4E-binding protein (4E-BP1). Activation of P70S6K leads to recruitment of the 40S ribosomal subunit to actively translating polysomes (17). In contrast, 4E-BP1 is a repressor of protein translation initiation, and phosphorylated 4E-BP1 dissociates from the initiation factor. Therefore, phosphorylation of 4E-BP1 via the mTOR pathway initiates protein translation (18, 19). These pathways that are regulated by mTOR activation enhance mRNA translation, which controls various physiologic processes in the cell, including growth, division, and metabolism (20, 21). In addition, Unc51-like kinase 1/2 (ULK1/2), which regulates the autophagy pathway, is a known target of mTOR. Thus, mTOR-signaling activity also modulates cell catabolism (22). Previous studies showed that molecular circadian clocks are

Authors' Affiliations: Departments of [1]Pharmaceutics and [2]Pharmaceutical Oncology, Graduate School of Pharmaceutical Sciences, Kyushu University, Fukuoka, Japan

Note: Supplementary data for this article are available at Cancer Research Online (http://cancerres.aacrjournals.org/).

H. Okazaki, N. Matsunaga, and S. Ohdo contributed equally to this work.

Corresponding Author: Shigehiro Ohdo, Department of Pharmaceutics, Graduate School of Pharmaceutical Sciences, Kyushu University, 3-1-1 Maidashi Higashi-ku, Fukuoka 812-8582, Japan. Phone: 81-92-642-6610; Fax: 81-92-642-6614; E-mail: ohdo@phar.kyushu-u.ac.jp

doi: 10.1158/0008-5472.CAN-12-3241

critical regulators of cell-cycle progression, cell homeostasis, and cell proliferation (23, 24). However, the relationship between the circadian clock and the mTOR-signaling pathway in tumor cells has not yet been determined.

In the present study, we investigated the 24-hour rhythm of mTOR signaling and its regulatory mechanism in tumor model mice. On the basis of the observed variations in mTOR-signaling activity, we tested whether the effect of an mTOR inhibitor (everolimus) is influenced by the dosing schedule.

Materials and Methods

Animals and cells

Five-week-old male BALB/c mice (Kyudo Co. Ltd.) were housed under a standard light/dark cycle at a temperature of 24°C ± 1°C and 60% ± 10% humidity with *ad libitum* access to food and water. RenCa, a mouse renal cell carcinoma cell line, was purchased from Cell Lines Service and cultured in RPMI-1640 supplemented with 10% FBS and 0.5% penicillin–streptomycin at 37°C in a 5% CO_2 atmosphere. A 25-μL aliquot containing 6×10^5 viable RenCa cells was injected into the right hind footpads of each mouse. The mice were used as a model after the tumors reached approximately 100 mm^3. Tumors were measured with a caliper, and the volume was calculated using the formula of an ellipsoid [$V = \pi/6\,(d1 \times d2 \times d3$), where $d1$, $d2$, and $d3$ represent the three diameters]. NIH3T3 cells were supplied by the Cell Resource Center for Biochemical Research, Tohoku University (Sendai, Japan). NIH3T3 cells were cultured under the same conditions as RenCa cells except for the culture medium, which was Dulbecco's Modified Eagle Medium. We confirmed that both cell lines were authenticated by each cell bank using STR–PCR analysis, and these cell lines were used in less than 3 months from frozen stocks. We confirmed that there was no microbial in both cell lines using fluorochrome staining.

Drug preparation

Everolimus (RAD001) was formulated at a concentration of 2% (w/v) in a microemulsion vehicle, which was purchased from Novartis Pharma AG. It was frozen after dilution in distilled water to the appropriate concentration. It was thawed immediately before use.

Experimental design

To observe the temporal expression profile of mTOR-related proteins in tumor cells, tumors were removed from the RenCa-bearing mice at six different time points (9:00, 13:00, 17:00, 21:00, 1:00, and 5:00) 12 days after implantation. The levels of mTOR, p-mTOR (Ser2448), p-P70S6K (Thr389), and LC3-II were measured by Western blotting, and *mTOR* mRNA levels were measured by quantitative reverse transcription PCR (qRT-PCR). To confirm the tumor homogeneity, mTOR activity in tissues obtained from normal footpads and tumors of the model mice at 1:00 was compared. Total proteins were extracted from these tissues, and protein expression was analyzed by Western blotting (Supplementary Fig. 1). To investigate the mechanism underlying the rhythmic variation of mTOR protein expression in tumor cells, Fbxw7 mRNA and protein levels were determined by qRT-PCR and Western blotting, respectively. To demonstrate the mechanism underlying the circadian rhythm of Fbxw7, the effect of the clock gene on the transcriptional activity of *Fbxw7* was assessed using the dual luciferase assay. To investigate the mechanism underlying the rhythmic expression of *Fbxw7*, a transfection experiment was performed using NIH3T3 cells in place of RenCa cells, because it was difficult to transfect RenCa cells with the expression vector and siRNA. To confirm the interaction between Fbxw7 and D-site–binding protein (DBP), endogenous DBP in NIH3T3 cells was knocked down with a siRNA. The DBP knockdown cells were treated with 50% FBS for 2 hours to synchronize their circadian clocks, and then the mRNA levels of *Dbp* and *Fbxw7* were assessed 32 and 44 hours after treatment. The circadian rhythms of DBP and E4BP4 in tumor masses were determined using RT-PCR and Western blotting. To investigate the temporal binding of endogenous DBP to the D-site in the mouse *Fbxw7* promoter, chromatin immunoprecipitation analysis was performed in individual tumors at 13:00 and 1:00. To assess the effect of the everolimus-dosing schedule on the survival of tumor-bearing mice, RenCa-implanted mice were administered 20 mg/kg everolimus i.v., and survival was assessed. To determine the effect of dosing time on the pharmacokinetics of everolimus, whole blood was collected at two different times after administration. The blood concentration of everolimus was determined by reverse phase high-performance liquid chromatography (RP-HPLC). Finally, to demonstrate whether the antitumor effect of everolimus is affected by the 24-hour rhythm of mTOR, cell viability was assessed by an ATP assay in serum-shocked RenCa cells.

Western blot analysis

Total protein was extracted from implanted RenCa tumors, normal footpads, liver, and cultured cells by using CelLytic MT Cell Lysis Reagent (Sigma-Aldrich) supplemented with protease inhibitor cocktail, which contains 2 μg/mL of aprotinin, 2 μg/mL of leupeptin, 100 μmol/L of phenylmethylsulfonylfluoride (PMSF), and 200 μmol/L of sodium vanadate. The protein concentration was determined using a BCA Protein Assay Kit (Pierce Biotechnology, Inc.). Lysate samples were separated on 7%, 10%, and 15% SDS–polyacrylamide gels and transferred to polyvinylidene difluoride membranes. The membranes were incubated with antibodies against mTOR, p-mTOR (Cell Signaling Technology), p-P70S6K (R&D Systems), FBXW7 (Abcam), DBP (Aviva Systems Biology LLC), LC3 (Novus Biologicals), cyclin D1, cyclin E, glyceraldehyde-3-phosphate dehydrogenase (GAPDH), and β-actin (Santa Cruz Biotechnology). The immunocomplexes were detected by incubation with horseradish peroxidase–conjugated secondary antibodies and were visualized using Chemi-Lumi One (Nacalai Tesque, Inc.). The membranes were photographed using Polaroid-type film or an Image Quant LAS-4000 (Fujifilm), and the density of each band was analyzed using the ImageJ software.

RT-PCR analysis

Total RNA was extracted from implanted RenCa tumors, liver, and cultured cells using RNAiso (Takara Bio). cDNA was

synthesized using the ReverTra Ace qPCR RT Kit (Toyobo). The cDNA levels of mouse *mTOR* (NM_020009), *Fbxw7* (NM_080428), *Dbp* (NM_016974), *E4bp4* (NM_017373), and 18S ribosomal RNA (rRNA; NR_003278) were determined by PCR. Real-time PCR analysis was performed on diluted cDNA samples using THUNDERBIRD SYBR qPCR Mix (Toyobo) with the 7500 Real-Time PCR System (Applied Biosystems). Semi-quantitative PCR was performed on diluted cDNA samples using the Gotaq Green Master Mix (Promega). Primer sequences are shown in Supplementary Fig. 2.

Construction of reporter plasmids

The 5′-flanking region of the mouse *Fbxw7* gene (−2,013 bp to +1 bp; +1 is the transcription start site) was amplified by Platinum PCR SuperMix High Fidelity (Invitrogen) using DNA extracted from mouse liver. PCR was performed using forward primer No. 1 [5′-AAACTCGAGTGCCTGGGTCATATGTAGAG-3′ (*Xho*I site underlined)] and reverse primer [5′-GGAAGATCTTTCAGCAATGCAGACTGCAC-3′ (*Bgl*II site underlined)]. PCR products were purified and ligated into a PGL4.12 basic vector (Fbxw7:Luc; full length). For the D-site deletion assay, two reporter vectors were constructed using forward primers No. 2 [−676 bp to +1 bp; 5′-GAACTCGAGCATGCATTAGGTA-GAAGTGG-3′ (*Xho*I site underlined)] and No. 3 [−364 bp to +1 bp; 5′-AAACTCGAGACTGCCCAAGCTACTTGAAG-3′ (*Xho*I site underlined)]. The same reverse primer (shown above) was used to construct these three reporter vectors.

Transfection and drug selection

RenCa cells were reverse transfected using Plus Reagent (Invitrogen) and Lipofectamine LTX Reagent (Invitrogen). The cells were transfected with pcDNA3.1 (Promega) or an Fbxw7 (addgene) expression vector (10 μg). Twenty-four hours after transfection, the cells were treated with G418 (2,000 μg/mL). Living cells were collected 72 hours after treatment.

Luciferase reporter assay

We used NIH3T3 cells for the transcriptional analysis of *Fbxw7* because transcriptional analysis using RenCa cells or other tumor cells is technically very difficult. NIH3T3 cells were seeded in culture plates at a density of 1×10^5 cells per well for the luciferase reporter assay. After 24 hours of culture, the cells were transfected with the reporter vector (100 ng) and the expression vector (1,500 ng) using Lipofectamine LTX reagent. To correct for variations in transfection efficiency, 0.125 ng of phRL-TK (Promega) was cotransfected in all experiments. The total amount of DNA per well was adjusted by adding pcDNA3.1 vector (Invitrogen). Twenty-four hours after transfection, the cells were harvested and the cell lysate was analyzed using the Dual Luciferase Reporter Assay System (Promega). In each sample, the luciferase activity from the reporter plasmid was normalized to *Renilla* luciferase activity.

Chromatin immunoprecipitation assays

Tumor masses were excised and treated with 8% formaldehyde for 10 minutes at room temperature to cross-link the chromatin, and the reaction was stopped by adding glycine at a final concentration of 0.125 mol/L. Each cross-linked sample was sonicated on ice and then incubated with antibodies against DBP. Chromatin–antibody complexes were extracted using a protein G agarose kit (Millipore). DNA was isolated using the Wizard SV Genomic DNA Purification System (Promega) and subjected to PCR using the following primers to amplify the DBP-binding site (D-site) in the *Fbxw7* promoter region: forward, 5′- CGAGAATCACTGGCAGTTA-3′ and reverse, 5′-CAAGTAGCTTGGGCAGTGTG-3′.

RNA interference

siRNA against the mouse *Dbp* gene was designed using the BLOCK-iT RNAi Designer (Invitrogen). The siRNA oligonucleotide sequences were as follows: control siRNA sense 5′-UUCCCAGGAAUACUCGAUUCCAACG-3′ and antisense 5′-CGUUGGAAUCGAG UAUUCCUGGGAA-3′; *Dbp* siRNA sense 5′-UUCAAAGGUCAUUAGCACCUCCACG-3′ and antisense 5′-CGUGGAGGUGCUAAUGACCUUUGAA-3′. These oligonucleotides were transfected into NIH3T3 cells using Lipofectamine RNAiMAX (Invitrogen).

Determination of everolimus concentration by HPLC

Whole blood samples were obtained from the heart at 0.5, 1, 2, 4, 12, and 24 hours after administration of 20 mg/kg of everolimus. To plot a standard curve, six concentrations of everolimus (156.25, 312.5, 625, 1,250, 2,500, and 5,000 ng/mL) were prepared in whole blood collected from mice that were not given the drug. Everolimus was extracted from blood according to a previously reported method (25). In the extraction process, 800 ng of ascomycin (Wako) was added to the whole blood samples as an internal standard. The extracts were diluted in 140 μL of the mobile phase (methanol:water:acetonitrile, 50:28:22), and then 90 μL of the diluted extract was injected to the HPLC system. The HPLC system consisted of an Alliance 2695 Separations Module (Waters) and a Waters 2998 PDA detector, with the detector set at a wavelength of 277 nm. Separation was performed on an XBridge C18 column (150 × 4.6 mm; 3.5-μm bead size), with the thermostatic chromatograph oven set at 55°C, and the flow rate was set at 1.0 mL/minute.

Evaluation of survival rate

Twelve days after the RenCa cells were inoculated into the footpads of mice, a single injection of everolimus (20 mg/kg, i.v.) was administered to tumor-bearing mice at 7:00 or 19:00, and the control solution was administered at 19:00. The survival of tumor model mice was observed for 6 weeks. Everolimus was only administered as a single injection at the beginning of the experiment, and no additional drug was given in this experiment.

Cell viability assays

RenCa cells were seeded at a density of 1×10^3 cells per well in a 96-well culture plate. Everolimus was added 24 or 32 hours after replacing the medium containing 50% FBS. Seventy-two hours after everolimus addition, intracellular ATP was determined as an indicator of cell viability using the Cell Titer Glo Luminescent Cell Viability Assay Kit (Promega).

Statistical analysis

ANOVA was used for multiple comparisons. The Scheffé test was used to compare two groups. The Student *t* test was used to compare two independent groups. The log-rank test was used for the survival assay. A *P* value of less than 0.05 was considered significant.

Results

Circadian variation of the mTOR-signaling pathway in RenCa tumor masses

To investigate whether the mTOR-signaling pathway shows a circadian rhythm in RenCa tumors, phosphorylated mTOR (p-mTOR), total mTOR, and phosphorylated P70S6K (p-P70S6K) protein levels were determined by Western blotting. As shown in Fig. 1A, both proteins showed a 24-hour rhythm and the peak at 1:00. The results suggest that mTOR-signaling activity could show a 24-hour rhythm and that this rhythm is caused by variation in mTOR protein expression levels. Phosphorylated P70S6K (p-P70S6K) and LC3-II protein levels were measured to determine whether the circadian rhythm is maintained downstream of the mTOR-signaling pathway. The autophagy marker LC3-II also showed a circadian rhythm, and its oscillation was opposite to that of the mTOR protein circadian rhythm in RenCa tumors (Fig. 1A). To investigate the mechanism underlying the circadian rhythm of the mTOR protein, we determined mTOR mRNA levels. RT-PCR analysis revealed that mRNA levels did not show a significant circadian rhythm (Fig. 1B). Therefore, we focused on mTOR protein degradation rather than the regulation of mTOR mRNA transcription.

Circadian expression of Fbxw7, an mTOR degradation factor

F-box and WD-40 domain protein 7 (Fbxw7) is a ubiquitin ligase E3. mTOR is degraded by the ubiquitin–proteasome pathway, and it has been shown that mTOR is ubiquitinated by Fbxw7 (26). In fact, the expression of the mTOR protein was low in RenCa cells transfected with the Fbxw7 expression vector (Fig. 2A). Therefore, we hypothesized that the 24-hour rhythm of the mTOR protein was caused by the rhythmic expression of Fbxw7. To confirm this hypothesis, we measured Fbxw7 mRNA and protein levels in RenCa-bearing mice. Fbxw7 mRNA and protein expression levels showed circadian rhythms and their oscillation patterns were antiphase of the circadian rhythm of the mTOR protein (Fig. 2B and C). These results suggest that the rhythm of the mTOR protein was dependent on the circadian rhythm of Fbxw7. Therefore, we investigated the circadian mechanism of Fbxw7 in the following experiments.

Fbxw7 transcription activity is regulated by DBP

To investigate how the circadian rhythm of *Fbxw7* mRNA is regulated, we constructed a luciferase reporter plasmid containing the proximal promoter of the mouse *Fbxw7* gene (Supplementary Fig. 3). The constructed vector contained two E-boxes and two D-site sequences, which are clock gene response elements, derived from the *Fbxw7* promoter. The dual luciferase assay showed that cells cotransfected with the *Fbxw7* luciferase reporter vector and DBP had high luciferase activity,

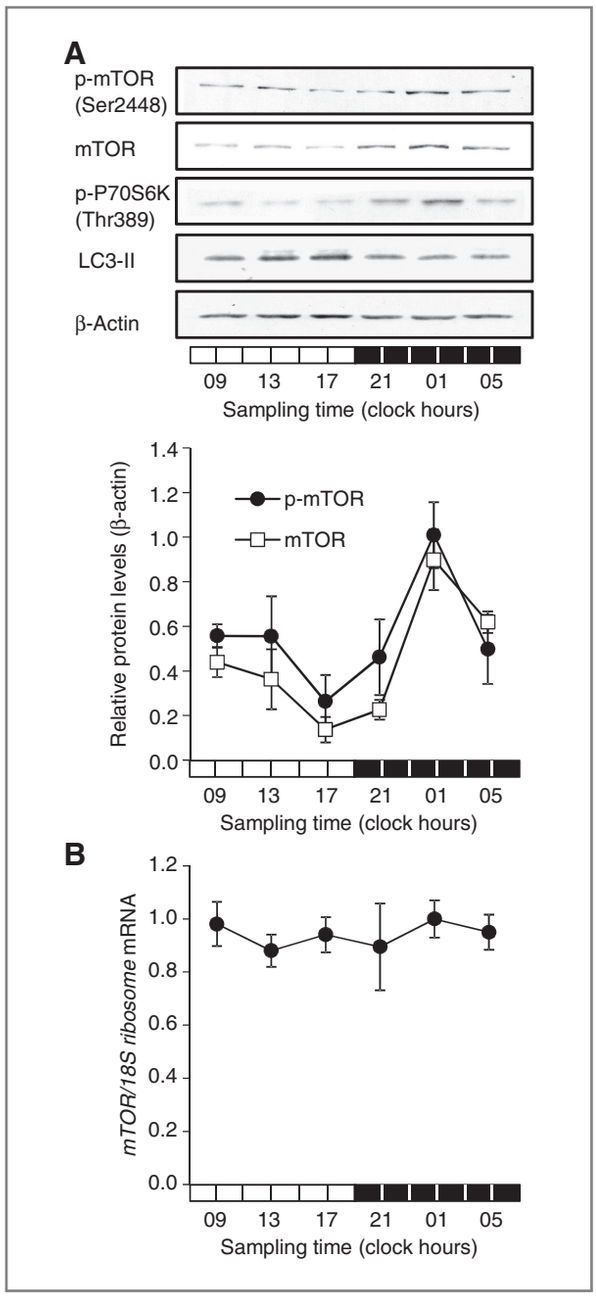

Figure 1. Temporal expression profile of mTOR in RenCa tumors. A, temporal expression profile of mTOR protein in tumor masses. The photographs show the 24-hour variation in mTOR, p-mTOR (Ser2448), p-P70S6K (Thr389), and LC3-II proteins in implanted RenCa tumor cells. Protein levels were measured by using specific antibodies for each protein. The bottom graph shows the relative mTOR and p-mTOR protein levels. The data were normalized using β-actin as a control. Values are shown as the means with the SEM ($n = 3$). Both proteins varied over a 24-hour period ($P < 0.05$, ANOVA). B, temporal expression profile of *mTOR* mRNA in tumors. Values are shown as the means with the SEM ($n = 3$).

whereas cells cotransfected with the *Fbxw7* luciferase reporter vector and CLOCK/BMAL1 or RORα had low luciferase activity (Fig. 3A). To investigate which D-site was important for the

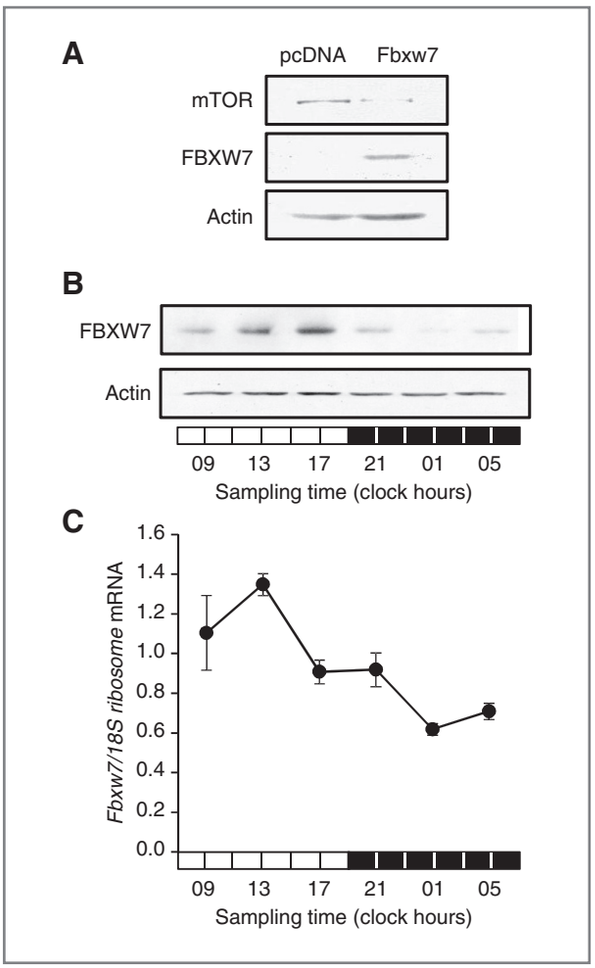

Figure 2. Temporal expression profile of Fbxw7 in RenCa tumors. A, the expression levels of mTOR and FBXW7 protein in pcDNA3.1- or Fbxw7-transfected RenCa cells selected by G418. RenCa cells were transfected with an expression plasmid (pcDNA3.1 or Fbxw7) by reverse transfection with Plus Reagent and Lipofectamine LTX. B, temporal expression of FBXW7 protein in tumors. Total protein was extracted at six different time points and protein levels were measured by Western blotting. C, temporal expression profile of *Fbxw7* mRNA in tumors. The data are normalized to 18S rRNA levels. Each point is the mean ± SEM of three mice ($P < 0.05$, ANOVA).

regulation of *Fbxw7* transcriptional activity, we constructed two luciferase reporter vectors with deletions (Fig. 3B, left). The dual luciferase assay revealed that cells cotransfected with the full-length luciferase reporter vector or the deletion-1 luciferase reporter vector and DBP had high luciferase activity, whereas cells cotransfected with the deletion-2 luciferase reporter vector and DBP had slightly increased luciferase activity compared with cells cotransfected with the deletion-2 luciferase reporter vector and pcDNA (Fig. 3B, right). These results suggest that the D-site element within −467 bp was important for *Fbxw7* transcriptional regulation. In addition, we used siRNA to knock down *Dbp* in serum-shocked NIH3T3 cells to confirm the influence of DBP on *Fbxw7* transcription. Consequently, *Fbxw7* mRNA levels were decreased by transfection of *Dbp* siRNA 44 hours after serum treatment (Fig. 4).

Time-dependent changes in the binding of endogenous DBP to the D-site element in the *Fbxw7* promoter

To confirm the hypothesis that DBP interacts with the *Fbxw7* promoter, we performed the following experiments. First, we determined *Dbp* and *E4bp4* mRNA levels in RenCa-bearing mice. As shown in Fig. 5A (left), *Dbp* mRNA levels showed a significant 24-hour rhythm in tumors. In contrast, *E4bp4* did not show rhythmic expression (Fig. 5A, right). DBP protein levels also showed a 24-hour rhythm in tumors (Fig. 5B). To investigate the temporal binding of endogenous DBP to the D-site element (−467 bp) in the *Fbxw7* promoter, we performed a chromatin immunoprecipitation assay. This assay revealed that more DBP was bound to the D-site element in the *Fbxw7* promoter at 13:00 than at 1:00 (Fig. 5C).

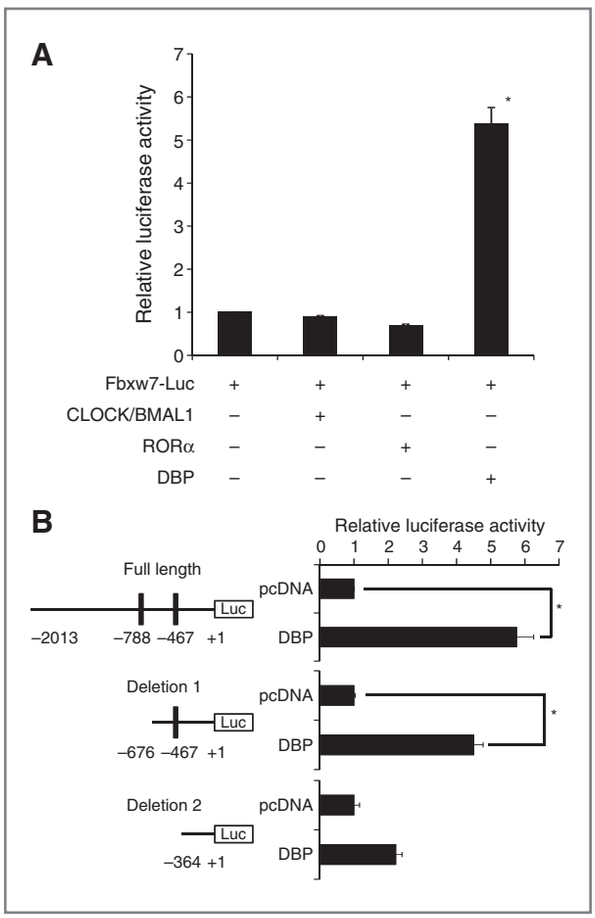

Figure 3. Influence of circadian clock genes on the transcription of *Fbxw7*. A, effect of clock genes on the luciferase activity of an *Fbxw7*-luciferase reporter. The mean value of the control (pcDNA) group was set at 1, and all values are shown as the fold increase compared with the value of the control. Each value is the mean ± SEM of three experiments. *, $P < 0.01$ versus the control group using the Scheffé test. B, luciferase activity of the full length or deletion reporter plasmids (Del.1 or Del.2) in the presence of DBP. Left, black bars indicate the D-site sequences. The mean value of the control (pcDNA) group was set at 1, and all values are shown as the fold increase compared with the value of the control. Each value is the mean ± SEM of three experiments. *, $P < 0.05$ versus the control group using the Scheffé test.

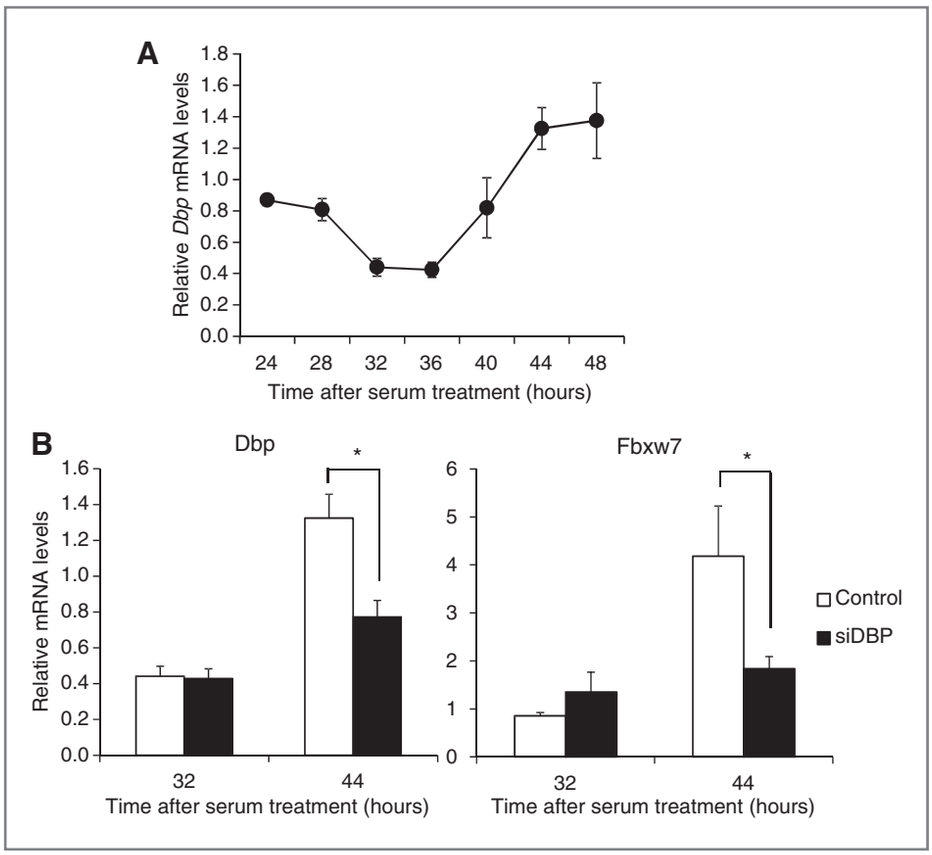

Figure 4. Influence of Dbp knockdown on Fbxw7 mRNA expression. A, the expression profiles of *Dbp* in serum-shocked NIH3T3 cells. The mRNA levels of *Dbp* were assessed by RT-PCR. The data are normalized to 18S rRNA as a control. Each value represents the mean ± SEM ($n = 3$, $P < 0.05$, ANOVA). B, the mRNA levels of *Dbp* and *Fbxw7* in siRNA-transfected NIH3T3 cells. Cells were treated with 50% FBS 12 hours after siRNA transfection, and total RNA was extracted at 32 or 44 hours after serum treatment. The mRNA levels were determined by real-time RT-PCR. The data are normalized to 18S rRNA as a control. Each value represents the mean ± SEM ($n = 3$). *, $P < 0.05$ control siRNA versus Dbp siRNA.

The influence of everolimus dosing time on the survival of tumor-bearing mice

The survival of tumor model mice was observed after administration of everolimus (20 mg/kg, i.v.) at 7:00 or 19:00. As shown in Fig. 6, the survival rate of mice administered everolimus at 19:00 was higher than that of mice administered everolimus at 7:00. To verify the influence of pharmacokinetics on survival, the everolimus concentration in blood was determined by HPLC after a single injection of everolimus (20 mg/kg) at two different times. There was no significant difference between the everolimus blood concentration in mice injected at 7:00 or 19:00 (Fig. 7).

Discussion

The mTOR-signaling pathway plays an important role in various cellular functions, including regulation of the immune response, neuropathic pain, and cancer cell proliferation. Recent studies have reported that various biologic functions show a 24-hour oscillation pattern in tumor cells, and that antitumor drugs exhibit a time-dependent effect (27, 28, 29). Moreover, these signaling oscillations are regulated by circadian clock systems. The control of circadian physiology relies on the interplay of interconnected transcription–translation feedback loops.

In this study, the protein levels of p-mTOR and p-P70S6K in RenCa cells implanted in mice showed 24-hour oscillation patterns (Fig. 1A). This result suggests that activity of the mTOR-signaling pathway also shows a circadian rhythm. In previous reports, it has been shown that mTOR regulates cell energy homeostasis via inhibition of autophagy (22). To investigate the presence of a diurnal rhythm downstream of the mTOR-signaling pathway, we measured the expression levels of the LC3-II protein, which is a known autophagy indicator. The temporal expression profiles of LC3-II showed a circadian rhythm in an antiphase manner of the circadian rhythm of mTOR-signaling activity. This result is consistent with previous studies showing that high mTOR activity suppressed the induction of autophagy. Furthermore, there is a diurnal rhythm in the activity of rodents; therefore, their food intake increases in the dark phase. mTOR signaling and autophagy regulation are directly correlated with nutrition signals; that is, the diurnal rhythm of mTOR may be regulated by plasma nutrient factors. In contrast, as shown in Fig. 1A, nearly all of the mTOR protein was phosphorylated. This was probably because the growth factors and nutrients present in the tumor tissues were more than enough to activate mTOR; thus, the fluctuation of mTOR protein was directly linked to the diurnal rhythm of mTOR signaling. Further study is required to elucidate the regulatory mechanism underlying the circadian rhythm of autophagy in tumor tissues.

Although mTOR protein abundance oscillated significantly in tumor tissues, *mTOR* mRNA levels were constant throughout the day (Fig. 1B). Therefore, we considered that the mTOR

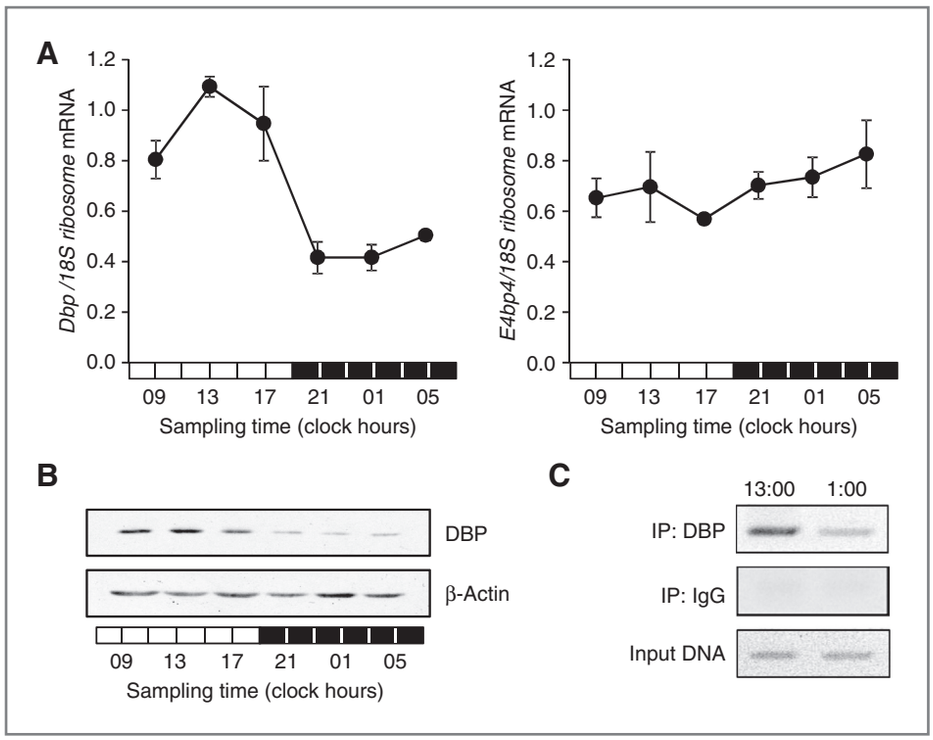

Figure 5. Time-dependent changes in the binding of endogenous DBP to the D-site element in the Fbxw7 promoter. A, temporal expression profiles of *Dbp* and *E4bp4* mRNA in tumors. The data are normalized to 18S rRNA as a control. Each point is the mean ± SEM of three mice. *Dbp* mRNA levels varied over a 24-hour period ($P < 0.05$, ANOVA). B, temporal expression of DBP protein in tumors was analyzed by Western blotting. Actin was used as an internal control. C, chromatin immunoprecipitation analysis of the *Fbxw7* promoter in RenCa-implanted mice. Input DNA was used as an internal control.

protein circadian rhythm was regulated via mTOR protein degradation. Recent reports have shown that FBXL3, an orphan member of the F-box protein family, regulates the circadian rhythm through degradation of PER and CRY (30, 31). These reports suggest that protein degradation via ubiquitin plays an important role in the regulation of circadian clocks. In recent studies, it has been shown that the mTOR protein is degraded by the ubiquitin–proteasome pathway through ubiquitination by Fbxw7, which ubiquitinates some cell-cycle regulators such as c-Myc, c-Jun, cyclin E1, and mTOR (32, 33). Thus, in this study, we estimated Fbxw7 mRNA and protein levels in RenCa-bearing mice, and these levels showed a circadian expression pattern, which oscillated out of phase with the circadian rhythm of the mTOR protein (Fig. 2). In

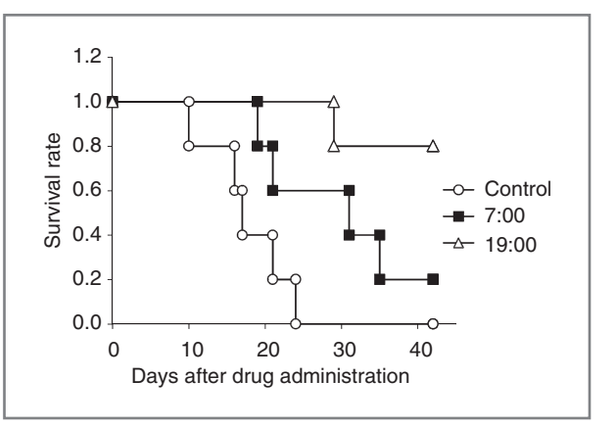

Figure 6. Influence of the dosing time of everolimus on the survival of tumor model mice. RenCa-bearing mice were administered (i.v.) a single dose of everolimus (20 mg/kg) at 7:00 (squares) or 19:00 (triangles). Similarly, control mice were administered (i.v.) with a placebo at 19:00 (open circles). The number of animals on day 0 (five mice) was set at 1, and all points are shown as a ratio of the number of animals compared with the number on day 0. There was a significant difference between the 19:00 administration group and the control group using the log-rank test.

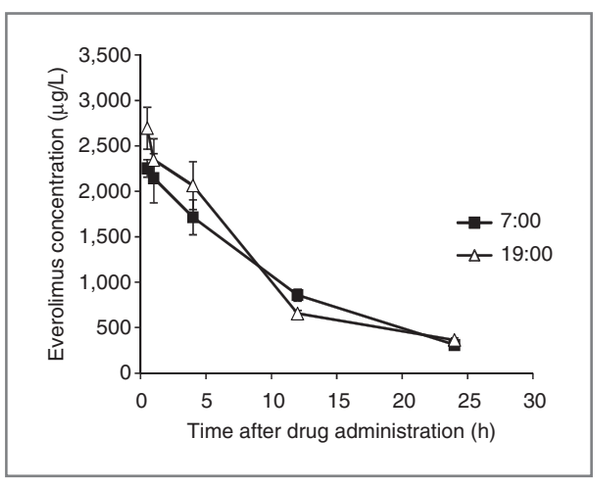

Figure 7. Everolimus blood concentration after administration at two different times. Blood levels of everolimus were monitored for 24 hours (0.5, 1, 2, 4, 12, and 24 hours) after administration. BALB/c mice were administered (i.v.) a single dose of everolimus at 7:00 (squares) or 19:00 (triangles). The concentration of everolimus in blood was determined as the ratio of the peak of everolimus to the peak of ascomycin (IS). Each point is the mean ± SEM of three mice.

contrast, as shown in Supplementary Fig. 4, the mTOR protein levels in the liver are higher in the dark phase than in the light phase, whereas Fbxw7 protein and mRNA levels varied very little throughout the day. As a result, the circadian rhythm of mTOR protein in mouse liver was regulated at the level of transcription. On the basis of these results, we hypothesized that the rhythmic oscillation of mTOR was due to rhythmic ubiquitination by Fbxw7.

We performed a dual luciferase assay to identify the clock-controlled genes that influence the circadian transcription of *Fbxw7*. The results of the luciferase assay suggested that the D-site at −467 bp plays an important role in DBP-mediated *Fbxw7* transcriptional regulation (Fig. 3). In addition, as shown in Fig. 4, the decrease of *Dbp* mRNA levels resulted in the disappearance of *Fbxw7* mRNA in cultured cells. DBP mRNA and protein levels in RenCa tumors showed a 24-hour expression pattern that was similar to that of *Fbxw7* mRNA. In contrast, E4BP4, which represses transcriptional activation by binding to the D-site, showed no significant circadian rhythm (Fig. 5). To verify that DBP binds to the D-site in the *Fbxw7* promoter in a time-dependent manner, we performed a chromatin immunoprecipitation assay. The results suggested that the *Fbxw7* mRNA circadian rhythm is mainly dependent on the circadian expression of DBP. On the basis of these results, we concluded that the 24-hour rhythm of mTOR activity is regulated by protein degradation that is controlled by Fbxw7 via circadian clock systems.

In this study, we used everolimus as an mTOR inhibitor to investigate whether the 24-hour oscillation of mTOR expression influences the drug's effect. Everolimus has been approved as a treatment for renal cell cancer, and it specifically inhibits mTOR activity. As shown in Fig. 6, the survival rate of tumor-bearing mice was higher when everolimus was administered at 19:00 than administered at 7:00. To confirm whether the difference in survival rate is caused by mTOR activity, we assayed the antiproliferative effect of everolimus on RenCa cells after 50% serum administration. In serum-shocked RenCa cells, mTOR activity was higher at 32 hours after serum treatment than at 24 hours. Relative cell viability was determined in RenCa cells exposed to everolimus 24 or 32 hours after serum shock. The antiproliferative effect was more potent in cells exposed to everolimus 32 hours after serum treatment than in cells exposed 24 hours after serum treatment (Supplementary Fig. 5). These results indicate that high levels of mTOR activation in RenCa tumors render them more sensitive to everolimus. In tumor model mice, the inhibition ratio of p-P70S6K at 6 hours after everolimus injection was higher following injection at 19:00 than at 7:00. Moreover, cyclin D1 was higher in the dark phase and was decreased by everolimus in the dark phase only. In contrast, cyclin E was weakly expressed in the dark phase and increased following everolimus injection at 19:00 (Supplementary Fig. 6). Cyclin D1, a cell-cycle regulator, is regulated via the mTOR-signaling pathway. Therefore, these results suggest that circadian variation in mTOR signaling and proteins downstream of mTOR signaling influences the therapeutic effect of everolimus. In addition, the similar rhythm of mTOR protein levels in normal liver and tumors is shown in Supplementary Fig. 4. However, mTOR-signaling activity in the liver was lower than in tumor tissues; therefore, we inferred that the effect of dosing time on non-tumor tissues is minor due to the lower levels of mTOR activity. These results suggest that the 24-hour oscillation of mTOR activity might influence the antitumor effect of mTOR inhibitors.

In recent years, chronopharmacologic strategies based on pharmacokinetics or pharmacodynamics have been developed. In the present study, we revealed that the 24-hour rhythm of mTOR-signaling activity in RenCa cells was regulated by DBP through degradation via the ubiquitin–proteasome pathway. In addition, the circadian accumulation of mTOR caused dosing time-dependent variation in the antitumor effect of everolimus. These findings showed that the novel regulatory mechanism underlying cell proliferation by circadian clock systems through the mTOR-signaling pathway is modulated by ubiquitination, and suggested that the potency of mTOR inhibitors could be improved by modulating the timing of administration.

Disclosure of Potential Conflicts of Interest

No potential conflicts of interest were disclosed.

Authors' Contributions

Conception and design: H. Okazaki, N. Matsunaga
Development of methodology: H. Okazaki, N. Matsunaga, S. Koyanagi
Acquisition of data (provided animals, acquired and managed patients, provided facilities, etc.): H. Okazaki, N. Matsunaga
Analysis and interpretation of data (e.g., statistical analysis, biostatistics, computational analysis): H. Okazaki, T. Fujioka, F. Okazaki, Y. Akagawa, S. Koyanagi
Writing, review, and/or revision of the manuscript: H. Okazaki, M. Ono, M. Kuwano, S. Ohdo
Administrative, technical, or material support (i.e., reporting or organizing data, constructing databases): H. Okazaki, Y. Akagawa, Y. Tsurudome
Study supervision: H. Okazaki, N. Matsunaga, M. Kuwano, S. Koyanagi, S. Ohdo

Acknowledgments

The authors thank the Research Support Center, Graduate School of Medical Sciences, Kyushu University, for technical support.

Grant Support

This study was supported in part by Grants-in-Aid for Scientific Research (A; 25253038; S. Ohdo), for Scientific Research on Innovative Areas (25136716; S. Ohdo), and for Challenging Exploratory Research (25670079; S. Ohdo) from the Japan Society for the Promotion of Science (JSPS).

The costs of publication of this article were defrayed in part by the payment of page charges. This article must therefore be hereby marked *advertisement* in accordance with 18 U.S.C. Section 1734 solely to indicate this fact.

Received August 15, 2012; revised October 15, 2013; accepted November 11, 2013; published OnlineFirst November 19, 2013.

References

1. Stephan FK, Zucker I. Circadian rhythms in drinking behavior and locomotor activity of rats are eliminated by hypothalamic lesions. Proc Natl Acad Sci U S A 1972;69:1583–6.
2. Gekakis N, Staknis D, Nguyen HB, Davis FC, Wilsbacher LD, King DP, et al. Role of the CLOCK protein in the mammalian circadian mechanism. Science 1998;280:1564–9.

3. Alvarez JD, Sehgal A. Circadian rhythms: finer clock control. Nature 2002;419:798–9.
4. Kume K, Zylka MJ, Sriram S, Shearman LP, Weaver DR, Jin X, et al. mCRY1 and mCRY2 are essential components of the negative limb of the circadian clock feedback loop. Cell 1999;98:193–205.
5. Sato TK, Panda S, Miraglia LJ, Reyes TM, Rudic RD, McNamara P, et al. A functional genomics strategy reveals Rora as a component of the mammalian circadian clock. Neuron 2004;43:527–37.
6. Wuarin J, Schibler U. Expression of the liver-enriched transcriptional activator protein DBP follows a stringent circadian rhythm. Cell 1990; 63:1257–66.
7. Sato TK, Yamada RG, Ukai H, Baggs JE, Miraglia LJ, Kobayashi TJ, et al. Feedback repression is required for mammalian circadian clock function. Nat Genet 2006;38:312–9.
8. Wood PA, Du-Quiton J, You S, Hrushesky WJ. Circadian clock coordinates cancer cell cycle progression, thymidylate synthase, and 5-fluorouracil therapeutic index. Mol Cancer Ther 2006;5:2023–33.
9. Levi F. Chronotherapeutics: the relevance of timing in cancer therapy. Cancer Causes Control 2006;17:611–21.
10. Lis CG, Grutsch JF, Wood P, You M, Rich I, Hrushesky WJ. Circadian timing in cancer treatment: the biological foundation for an integrative approach. Integr Cancer Ther 2003;2:105–11.
11. Ohdo S. Changes in toxicity and effectiveness with timing of drug administration: implications for drug safety. Drug Saf 2003;26: 999–1010.
12. Nave BT, Ouwens M, Withers DJ, Alessi DR, Shepherd PR. Mammalian target of rapamycin is a direct target for protein kinase B: identification of a convergence point for opposing effects of insulin and amino-acid deficiency on protein translation. Biochem J 1999;344:427–31.
13. Grewe M, Gansauge F, Schmid RM, Adler G, Seufferlein T. Regulation of cell growth and cyclin D1 expression by the constitutively active FRAP-p70s6K pathway in human pancreatic cancer cells. Cancer Res 1999;59:3581–7.
14. Seufferlein T, Rozengurt E. Rapamycin inhibits constitutive p70s6k phosphorylation, cell proliferation, and colony formation in small cell lung cancer cells. Cancer Res 1996;56:3895–7.
15. Boulay A, Zumstein-Mecker S, Stephan C, Beuvink I, Zilbermann F, Haller R, et al. Antitumor efficacy of intermittent treatment schedules with the rapamycin derivative RAD001 correlates with prolonged inactivation of ribosomal protein S6 kinase 1 in peripheral blood mononuclear cells. Cancer Res 2004;64:252–61.
16. Pitt M, Crathorne L, Moxham T, Bond M, Hyde C. Everolimus for the second-line treatment of advanced and/or metastatic renal cell cancer: a critique of the submission from Novartis. Health Technol Assess 2010;14 Suppl 2:41–6.
17. Ruvinsky I, Meyuhas O. Ribosomal protein S6 phosphorylation: from protein synthesis to cell size. Trends Biochem Sci 2006;31:342–8.
18. Haghighat A, Mader S, Pause A, Sonenberg N. Repression of cap-dependent translation by 4E-binding protein 1: competition with p220 for binding to eukaryotic initiation factor-4E. EMBO J 1995; 14:5701–9.
19. Hara K, Yonezawa K, Kozlowski MT, Sugimoto T, Andrabi K, Weng QP, et al. Regulation of eIF-4E BP1 phosphorylation by mTOR. J Biol Chem 1997;272:26457–63.
20. Peterson TR, Sengupta SS, Harris TE, Carmack AE, Kang SA, Balderas E, et al. mTOR complex 1 regulates lipin 1 localization to control the SREBP pathway. Cell 2011;146:408–20.
21. Finger DC, Salama S, Tsou C, Harlow E, Blenis J. Mammalian cell size is controlled by mTOR and its downstream targets S6K1 and 4EBP1/eIF4E. Genes Dev 2002;16:1472–87.
22. Meijer AJ, Codogno P. Regulation and role of autophagy in mammalian cells. Int J Biochem Cell Biol 2004;36:2445–62.
23. Khapre RV, Samsa WE, Kondratov RV. Circadian regulation of cell cycle: molecular connections between aging and the circadian clock. Ann Med 2010;42:404–15.
24. Miyazaki K, Wakabayashi M, Hara Y, Ishida N. Tumor growth suppression *in vivo* by overexpression of the circadian component, PER2. Genes Cells 2010;15:351–8.
25. Khoschsorur G. Simultaneous measurement of sirolimus and everolimus in whole blood by HPLC with ultraviolet detection. Clin Chem 2005;51:1721–4.
26. Mao JH, Kim IJ, Wu D, Climent J, Kang HC, DelRosario R, et al. FBXW7 targets mTOR for degradation and cooperates with PTEN in tumor suppression. Science 2008;321:1499–502.
27. Nakagawa H, Takiguchi T, Nakamura M, Furuyama A, Koyanagi S, Aramaki H, et al. Basis for dosing time-dependent change in the anti-tumor effect of imatinib in mice. Biochem Pharmacol 2006;72: 1237–45.
28. Kuramoto Y, Hata K, Koyanagi S, Ohdo S, Shimeno H, Soeda S. Circadian regulation of mouse topoisomerase I gene expression by glucocorticoid hormones. Biochem Pharmacol 2005;71:1155–61.
29. Koyanagi S, Kuramoto Y, Nakagawa H, Aramaki H, Ohdo S, Soeda S, et al. A molecular mechanism regulating circadian expression of vascular endothelial growth factor in tumor cells. Cancer Res. 2003; 63:7277–83.
30. Busino L, Bassermann F, Maiolica A, Lee C, Nolan PM, Godinho SI, et al. SCFFbxl3 controls the oscillation of the circadian clock by directing the degradation of cryptochrome proteins. Science 2007; 316:900–4.
31. Siepka SM, Yoo SH, Park J, Song W, Kumar V, Hu Y, et al. Circadian mutant overtime reveals F-box protein FBXL3 regulation of cryptochrome and period gene expression. Cell 2007;129:1011–23.
32. Koepp DM, Schaefer LK, Ye X, Keyomarsi K, Chu C, Harper JW, et al. Phosphorylation-dependent ubiquitination of cyclin E by the SCFFbw7 ubiquitin ligase. Science 2001;294:173–7.
33. Yada M, Hatakeyama S, Kamura T, Nishiyama M, Tsunematsu R, Imaki H, et al. Phosphorylation-dependent degradation of c-myc is mediated by the F-box protein Fbw7. EMBO J 2004;23:2116–25.